

Structural-informed functional MRI analysis of patients with empathy impairment following stroke

Jian-Feng Qu, MS, MD; Xiao-Wen Liu, MD; Ming-Zi Wang, MD; Yi-Shan Luo, PhD; Ting Gao, PhD; Lin Shi*, PhD; Yang-Kun Chen*, MD, PhD

Background: The underlying functional alterations of brain structural changes among patients with empathy impairment following stroke remain unclear. We sought to investigate functional connectivity changes informed by brain structural abnormalities in multimodal magnetic resonance imaging (MRI) among patients with empathy impairment following stroke. **Methods:** We enrolled people who had experienced their first ischemic stroke, along with healthy controls. We assessed empathy 3 months after stroke using the Chinese version of the Empathy Quotient (EQ). During the acute phase, all patients underwent basic magnetic resonance imaging (MRI), followed by multimodal MRI during follow-up. Our MRI analyses encompassed acute infarction segmentation, volumetric brain measurements, regional quantification of diffusion parameters, and both region-of-interest-based and seed-based functional connectivity assessments. We grouped patients based on the severity of their empathy impairment for comparative analysis. **Results:** We included 84 patients who had stroke and 22 healthy controls. Patients had lower EQ scores than controls. Patients with low empathy had larger left cortical infarcts (odds ratio [OR] 4.082, 95% confidence interval [CI] 1.183–14.088), more pronounced atrophy in the right cingulate cortex (OR 1.248, 95% CI 1.038–1.502), and lower scores on the Montreal Cognitive Assessment (OR 0.873, 95% CI 0.74–0.947). In addition, the cingulate cortex served as the seed in the seed-based analysis, which showed heightened functional connectivity between the anterior cingulate gyrus and the right superior parietal lobule, specifically in the low-empathy group. **Limitations:** We did not evaluate the relationship between specific network involvement and empathy impairment among patients following stroke. **Conclusion:** Among patients with subacute ischemic stroke, reduced empathy was strongly associated with a more severe cognitive profile and atrophy of the right cingulate cortex. Our subsequent structural-informed functional MRI analysis suggests that the enhanced connectivity between the anterior cingulate gyrus and the superior parietal lobule may function as a compensatory mechanism for this atrophy.

Introduction

Empathy refers to the ability of an individual to cognitively perceive, grasp, and understand the emotions and feelings of others; it requires one to stand in the other person's shoes to understand their emotions, thoughts, position, and feelings.^{1,2} Empathy plays a crucial role in prosocial behaviour, the inhibition of aggression, and moral reasoning by enabling people to understand the psychological states and emotions of others.³ Neurological and neuropsychiatric diseases — such as autism, frontotemporal dementia, traumatic brain injury, schizophrenia, and stroke — are known to impair empathy.⁴

After a stroke, patients may have impaired empathy and reduced perspective-taking abilities.⁵ Advanced imaging techniques can offer detailed and objective data for investigating the pathophysiology of empathy. Our pilot multimodal magnetic

resonance imaging (MRI) study involving patients with subacute ischemic stroke found that empathy impairment was negatively and positively correlated with right cortical infarction and putamen volume, respectively.⁶ Previous studies have identified numerous brain regions involved in empathy, including the anterior cingulate cortex (ACC), anterior insula, inferior parietal lobe, premotor cortex, posterior superior temporal sulcus, medial prefrontal cortex, posterior cingulate cortex, precuneus, temporal pole, and temporoparietal junction.⁷ Ziaei and colleagues⁸ found that older adults with quicker empathic responses to negative emotions had greater fractional anisotropy in the ACC, while those with quicker responses to positive emotions had greater fractional anisotropy in the posterior cingulum. In addition, activations in regions such as the anterior insula and the anterior and mid-cingulate cortex have been linked to pain-related empathy.⁹

Correspondence to: Yang-Kun Chen, Department of Neurology, The Tenth Affiliated Hospital of Southern Medical University (Dongguan People's Hospital), Dongguan, Guangdong Province, China; cykun78@163.com

*Lin Shi and Yang-Kun Chen contributed equally to this study.

Submitted July 28, 2024; Revised Aug. 27, 2024; Accepted Sept. 3, 2024

Cite as: *J Psychiatry Neurosci* 2024 October 25;49(5). doi: 10.1503/jpn.240084

Functional imaging studies have identified the brain networks involved in empathy. A quantitative meta-analysis of functional MRI (fMRI) studies concluded that the dorsal ACC, anterior midcingulate cortex–supplementary motor area, and bilateral insula constituted a core empathy network, distinguishing cognitive–evaluative from affective–perceptual empathy at the level of regional activation.¹⁰ Another resting-state fMRI (rs-fMRI) study of neurologically healthy adults found that affective empathy correlated with functional connectivity between the ventral anterior insula, orbitofrontal cortex, amygdala, and ACC, while cognitive empathy correlated with connectivity between the brainstem, superior temporal sulcus, and ventral anterior insula.¹¹

Stroke-induced lesions can disrupt canonical resting-state large-scale brain networks.¹² However, few imaging studies have simultaneously evaluated structural and functional abnormalities related to empathy after stroke. A small-scale study analyzed the association between infarcts and the hypothesized empathy network, particularly focusing on the temporal pole and anterior insula, among people with acutely impaired affective empathy.¹³ Investigating imaging evidence that reveals the effect of synchronized structural and functional changes on empathy among patients who have had a stroke can provide new insights into the mechanisms underlying empathy. In this study, we sought to explore the mechanisms of empathy impairment following stroke (i.e., low empathy) using a structural-guided functional analysis approach with multimodal MRI data.

Methods

Participants

We recruited participants from the Division I, Department of Neurology, at the Tenth Affiliated Hospital of Southern Medical University (Dongguan People's Hospital) between July 1, 2021, and Dec. 30, 2022. We included people aged 18 years or older who had had their first-ever acute ischemic stroke within 7 days before admission, defined as a sudden onset of neurologic dysfunction of any severity attributed to focal cerebral ischemia with or without imaging or laboratory evidence.¹⁴ Patients must have had a mild stroke (National Institutes of Health Stroke Scale [NIHSS] score ≤ 15 on admission) and good recovery with a modified Rankin Scale (mRS) score of 2 or less at discharge. Included patients had availability of complete multimodal brain MRI data according to the study protocol.

We excluded patients with incomplete MRI data; negative findings on diffusion-weighted imaging; hemorrhagic transformation; death during hospital admission; presence of severe comorbidities, such as malignant tumours or severe organ dysfunction; medical records indicating a history of dementia, mental disorders, severe depression, or evidence of serious cognitive dysfunction at admission; and refusal to sign the informed consent form.

We recruited healthy controls with no history of illness, matched by age and gender with the patient group.

Demographic and clinical variables were recorded for each participant. The attending neurologist determined the ischemic

stroke subtype according to the Trial of ORG 10172 in Acute Stroke Treatment (TOAST) classification system during hospital admission.¹⁵

All participants underwent follow-up exams 3 months (± 2 wk) after the index stroke using face-to-face interviews. We assessed empathy status using the Chinese version of the Empathy Quotient (EQ),¹⁶ which was translated from the original EQ and validated accordingly (Appendix 1, Figure 1, available at www.jpn.ca/lookup/doi/10.1503/jpn.240084/tab-related-content).¹⁷ The EQ consists of 60 questions, including 40 questions measuring empathy and 20 filler items. We included the filler items (items 2, 3, 5, 7, 9, 13, 16, 17, 20, 23, 24, 30, 31, 33, 40, 45, 47, 51, 53, and 56) to obscure the study's focus.

We abandoned an initial attempt to separate the items into purely affective and cognitive categories because, in most instances, the affective and cognitive components of empathy co-occur and cannot be easily disentangled. To avoid response bias, around half of the items were worded to elicit a “disagree” response and the other half to elicit an “agree” response for the empathy-related questions. For the questions measuring empathy, “definitely agree” responses received 2 points, and “slightly agree” responses received 1 point for items 1, 6, 19, 22, 25, 26, 35, 36, 37, 38, 41, 42, 43, 44, 52, 54, 55, 57, 58, 59, and 60. Conversely, “definitely disagree” responses received 2 points, and “slightly disagree” responses received 1 point for items 4, 8, 10, 11, 12, 14, 15, 18, 21, 27, 28, 29, 32, 34, 39, 46, 48, 49, and 50. The total EQ score ranges from 0 to 80, with higher scores indicating greater empathy.¹⁶

We conducted other psychological tests during the follow-up examination. We assessed cognition using the Montreal Cognitive Assessment (MoCA),¹⁸ anxiety using the Hamilton Anxiety Rating Scale (HARS), depression using the Hamilton Depression Rating Scale (HDRS), and sleeping status using the Pittsburgh Sleep Quality Index (PSQI). We also recorded the NIHSS score, mRS score, recurrence of stroke, and death during the follow-up period.

Imaging

We obtained brain MRI data using a 3.0 T MRI scanner (Skyra, Siemens). All patients underwent a basic MRI protocol, including T_1 -weighted, T_2 -weighted, and diffusion-weighted imaging in the acute stage. In the follow-up, all participants (including healthy controls) underwent multimodal MRI, which included additional 3-dimensional T_1 -weighted imaging, diffusion tensor imaging, and rs-fMRI alongside the basic MRI protocol. The acquisition parameters for the multimodal MRI are detailed in Appendix 2, Table 1, available at www.jpn.ca/lookup/doi/10.1503/jpn.240084/tab-related-content.

Post-processing

We analyzed MRI data using the fully automatic software AccuBrain (BrainNow Medical Technology). Structural information included infarct lesions, which were automatically segmented based on acute-stage diffusion-weighted images using

a deep-learning model; brain volumes of various subcortical structures, ventricles, and cortical lobar atrophy, quantified on the 3-dimensional T_1 -weighted images using a multi-atlas image registration scheme;¹⁹ and the microstructural integrity of the white matter, which was analyzed using diffusion tensor imaging, computing the mean fractional anisotropy and mean diffusivity in the participant's native space. Regional mean values of fractional anisotropy and mean diffusivity were quantified after mapping with the ICBM DTI-81 Atlas.²⁰

We assessed functional information of the brain by functional connectivity analysis, performed using the CONN toolbox 20b.²¹ We preprocessed all rs-fMRI data, which involved realignment with correction for susceptibility distortion interactions, slice timing correction, outlier detection, direct segmentation, normalization to the Montreal Neurological Institute template space, and smoothing. The functional data were denoised using a standard pipeline that included regression of potential confounding effects characterized by white-matter time series, cerebrospinal fluid (CSF) time series, motion parameters and their first-order derivatives, outlier scans, session and task effects and their first-order derivatives, and linear trends within each functional run. This was followed by bandpass frequency filtering of the BOLD time series between 0.01 Hz and 0.1 Hz. We used linear regression of confounding effects of white matter. We used linear regression to remove confounding factors of BOLD signal variation, including white-matter signals, CSF signals, realignment, scrubbing, and effect of rest.

Since there is no universally accepted cut-off point for EQ scores, we categorized participants into 3 groups based on the interquartile range of EQ scores. Those with EQ scores below the 25th percentile were designated as the low-empathy group, those with scores in the 25th–75th percentiles were designated as the moderate-empathy group, and those with scores greater than the 75th percentile were designated as the high-empathy group. Before exploring the functional connectivity changes related to varying levels of empathy, we analyzed preprocessed rs-fMRI data using analysis based on 2 regions of interest (ROIs) and seed-based analysis. In the ROI-based analysis, we estimated connectivity matrices between each pair of ROIs (using the FSL Harvard–Oxford atlas and automated anatomical labelling atlas) to characterize functional connectivity patterns. We performed group-level analyses using a general linear model. A separate general linear model was estimated for each voxel, with first-level connectivity measures at this voxel as dependent variables, and groups or other subject-level identifiers as independent variables. We tested other voxel-level hypotheses using multivariate parametric statistics with random-effects across participants and sample covariance estimation across multiple measurements. We performed inferences at the level of individual clusters, with cluster-level inferences based on parametric statistics from Gaussian random field theory. We corrected p values using the false discovery rate (FDR) and used a cluster-size threshold of less than 0.05.

We also conducted a seed-based analysis for regions with structural abnormalities. We identified specific structural abnormalities as seeds using a multivariate logistic regression

model, with low empathy serving as the independent variable. Subsequently, we performed seed-based analyses comparing the low-empathy group with the high-empathy and control groups. We computed the mean time series within each ROI and calculated the correlation between the average time series and the BOLD time series at each voxel. Group-level comparisons used parametric statistics based on random field theory, with an FDR-corrected $p < 0.05$ cluster-level significance threshold among the resulting clusters.

Statistical analysis

We conducted all statistical analyses using IBM SPSS for Windows (version 27.0). We performed both multivariate logistic regression and univariate analyses. We presented descriptive data as proportions, means, or medians, as appropriate. We conducted comparisons between the empathy groups using analysis of variance (ANOVA) for continuous variables with normal distribution, the Kruskal–Wallis test for continuous variables with skewed distribution, and the χ^2 test for categorical variables.

Univariate analyses compared clinical variables, structural volumetry for various brain regions, brain structural atrophy index, and microstructural integrity of the white matter between patients in different empathy groups. If the correlations between any of these putative risk factors was at least 0.40, we performed additional analyses to rule out collinearity.

To investigate potential risk factors associated with low empathy, we used a binary logistic regression model incorporating a backward elimination procedure, with low empathy serving as the dependent variable. We interpreted the odds ratio (OR) of any independent risk factor as indicating a risk of low empathy when all other risk factors were held constant. We set the 2-sided significance level at 0.05.

Ethics approval

The study protocol was approved by the ethics committee of Dongguan People's Hospital. We obtained informed consent from all participants in accordance with the Declaration of Helsinki.

Results

We enrolled a total of 84 patients who had their first acute ischemic stroke, as well as 22 healthy controls for comparison (Appendix 2, Figure 1, available at www.jpn.ca/lookup/doi/10.1503/jpn.240084/tab-related-content). The patients had an average age of 60.5 (standard deviation 9.7) years, and 64.3% were male (Table 1). In the whole sample, median scores were 37.5 (interquartile range [IQR] 30–48) on the EQ, 22 (IQR 18–25) on the MoCA, 3.5 (IQR 2–6) on the HARS, 5 (IQR 2–10) on the HDRS, and 5 (IQR 2.25–8) on the PSQI. Among patients, median EQ scores were 23.5 (IQR 20–26.25) in the low-empathy group, 38.5 (IQR 33–44) in the moderate-empathy group, and 52 (IQR 50.25–60) in the high-empathy group. Patients with low empathy were significantly more prone to have a history of atrial fibrillation or left cortical infarcts, and they also had lower

Table 1: Participant characteristics

Variable	No. (%) of participants*				p value
	Low empathy n = 22	Moderate empathy n = 42	High empathy n = 20	Healthy controls n = 22	
Age, yr, mean ± SD	62.7 ± 8.6	60.9 ± 9.2	57.3 ± 9.7	59.4 ± 6.0	0.2
Sex, male	16 (72.7)	28 (66.7)	10 (50.0)	10 (45.5)	0.2
NIHSS, median (IQR)					
On admission	2 (0.75–6)	2 (0–3.25)	2 (0.25–3)		0.8
On discharge	1 (0–1.25)	1 (0–2)	1 (0–2.75)		0.7
Hypertension	14 (63.6)	34 (81.0)	17 (85.0)		0.2
Diabetes	3 (13.6)	13 (32.0)	4 (20.0)		0.3
Atrial fibrillation	5 (22.7)	1 (2.4)	1 (5.0)		0.02
Thrombolysis	5 (22.7)	4 (9.5)	3 (15)		0.4
Mechanical thrombectomy	3 (13.6)	3 (7.1)	2 (10.0)		0.7
TOAST stroke subtype					0.3
Large artery atherosclerosis	7 (31.8)	15 (35.7)	9 (45.0)		
Cardioembolism	6 (27.3)	3 (7.1)	2 (10.0)		
Small artery occlusion	9 (40.9)	18 (42.9)	8 (40.0)		
Location of infarcts					
Left cortical	12 (54.5)	11 (26.2)	2 (10.0)		0.005
Right cortical	9 (40.9)	9 (21.4)	4 (20.0)		0.2
Left subcortical	9 (40.9)	17 (40.5)	7 (35.0)		0.9
Right subcortical	7 (31.8)	15 (35.7)	6 (30.0)		0.9
Infratentorial	4 (18.2)	10 (23.8)	6 (30.0)		0.7
Infarct volume, mean ± SD	8.3 ± 17.9	2.2 ± 3.7	2.7 ± 5.3		0.06
SBI, median (IQR)	8 (3.5–14.75)	9.5 (1.75–18)	9 (2–16.5)		1.0
EPVS, median (IQR)	1 (0–1.25)	1.5 (1–2)	1 (0.25–2)		0.2
CHIPS, median (IQR)	10 (0.75–26)	9 (1–21.5)	6 (1.25–14)		0.8
WMH volume, mean ± SD	7.3 ± 6.0	10.6 ± 15.6	7.2 ± 10.3		0.5
PVH volume, mean ± SD	5.8 ± 5.2	9.5 ± 15.5	6.3 ± 9.9		0.4
DWMH volume, mean ± SD	1.5 ± 1.1	1.1 ± 1.2	0.9 ± 0.9		0.2
EQ, median (IQR)	23.5 (20–26.25)	38.5 (33–44)	52 (50.25–60)		< 0.001
MoCA, mean ± SD	17.6 ± 4.8	22 ± 4.5	23.6 ± 4.2		< 0.001
HARS, mean ± SD	4.9 ± 3.9	4.3 ± 3.5	4.8 ± 4.8		0.8
HDRS, mean ± SD	7.7 ± 6.3	6.8 ± 5.9	4.3 ± 3.8		0.1
PSQI, mean ± SD	5.6 ± 3.1	5.5 ± 4.4	5.9 ± 3.7		0.9
mRS, median (IQR)	1 (0–1)	1 (0–1)	0 (0–1)		0.6

CHIPS = cholinergic pathways hyperintensities scale; DWMH = deep white-matter hyperintensities; EPVS = enlarged perivascular spaces; EQ = Empathy Quotient; HARS = Hamilton Anxiety Rating Scale; HDRS = Hamilton Depression Rating Scale; IQR = interquartile range; MoCA = Montreal Cognitive Assessment; mRS = modified Rankin Scale; NIHSS = National Institutes of Health Stroke Scale; PSQI = Pittsburgh Sleep Quality Index; PVH = periventricular hyperintensities; SBI = silent brain infarctions; SD = standard deviation; TOAST = Trial of ORG 10172 in Acute Stroke Treatment; WMH = white-matter hyperintensities.

*Unless indicated otherwise.

MoCA scores. There were no significant differences in HARS, HDRS, PSQI, and mRS scores between the empathy groups, nor did groups differ significantly on sex, NIHSS score on admission, and TOAST subtype. Patients had lower EQ scores (median 37.5, IQR 30–48) than controls (median 47, IQR 42–56.25, $p < 0.001$), as shown in Table 2.

The distribution of infarct lesions across empathy groups is illustrated in Figure 1. Notably, patients with lower empathy were more likely to have infarcts in the left hemisphere than those with higher empathy.

Structural information

In the univariate analyses, we compared the differences in clinical data, brain structure characteristics, and structural

connectivity between empathy groups. Patients with low empathy exhibited more pronounced atrophy in the left occipital lobe, left temporal lobe, and right cingulate cortex than those in other empathy groups (Table 3). No significant empathy-related differences were observed in total or unilateral brain structure volume, amygdala volume, or hypothalamus volume (Table 4 and Table 5). However, compared with controls, patients generally had smaller brain volumes (Table 6).

In the univariate analyses of categorized empathy and regional quantification of diffusion parameters, patients with low empathy, in contrast to those with high empathy, demonstrated significantly lower fractional anisotropy within the body of the corpus callosum, fornix, left superior fronto-occipital fasciculus, left uncinate fasciculus, and

right tapetum (Table 7). Furthermore, compared with patients with high empathy, patients with low empathy showed increased mean diffusivity in the fornix, right tapetum, and left tapetum. Compared with controls, patients demonstrated significantly lower fractional anisotropy and higher mean diffusivity in certain fibre tracts (Appendix 1, Table 2).

The results of the binary logistic regression models are presented in Table 8. After eliminating collinearity (Appendix 1, Table 3), our analysis incorporated variables such as atrial fibrillation, left cortical infarcts, atrophy of the right cingu-

late, integrity of the white matter, and MoCA scores (Figure 2). Based on the univariate analysis, we constructed 2 models to analyze the relationship between structural connectivity and low empathy. These models specifically evaluated the effect of mean diffusivity in the right tapetum or fractional anisotropy of the fornix, while keeping all other variables constant. Neither of these 2 factors exhibited a significant correlation with low empathy. Patients with low empathy were more likely to have left cortical infarcts (model 1 OR 4.082, 95% confidence interval [CI] 1.183–14.088), more pronounced atrophy of the right cingulate cortex (model 1 OR 1.248, 95% CI 1.038–1.502), and lower MoCA scores (model 1 OR 0.873, 95% CI 0.74–0.947).

Table 2: Comparison of assessments of patients after stroke and healthy controls

Assessment	Median (IQR)		z	p value
	Post-stroke patients n = 84	Healthy controls n = 22		
EQ	37.5 (30–48)	47 (42–56.25)	–3.523	< 0.001
MoCA	22 (18–25)	25 (22–26.25)	–2.668	< 0.001
HARS	3.5 (2–6)	3.5 (2–6)	–0.404	0.7
HDRS	5 (2–10)	3 (0–4)	–3.128	0.002
PSQI	5 (2.25–8)	2.5 (1–5.5)	–2.451	0.01

EQ = Empathy Quotient; HARS = Hamilton Anxiety Rating Scale; HDRS = Hamilton Depression Rating Scale; IQR = interquartile range; MoCA = Montreal Cognitive Assessment; mRS = modified Rankin Scale; PSQI = Pittsburgh Sleep Quality Index.

Functional connectivity among patients with low empathy

When comparing the low- and high-empathy groups using ROI-based analysis, we did not identify any significant correlations between any ROIs. However, in the subsequent seed-based analysis, with the ACC and posterior cingulate gyrus serving as seeds, we identified a significant cluster (coordinates +36 x, –50 y, +44 z). This cluster encompassed 136 (69%) voxels that covered 9% of the right superior parietal lobule, 28 (14%) voxels that covered 2% of the right angular gyrus, 9 (5%) voxels that covered 1% of the right superior lateral occipital cortex, and 7 (4%) voxels that covered 1% of the right posterior supramarginal gyrus (Figure 3 and Appendix 1, Figure 2). A comparison of the low-empathy group and controls yielded comparable results (Appendix 1, Figure 3).

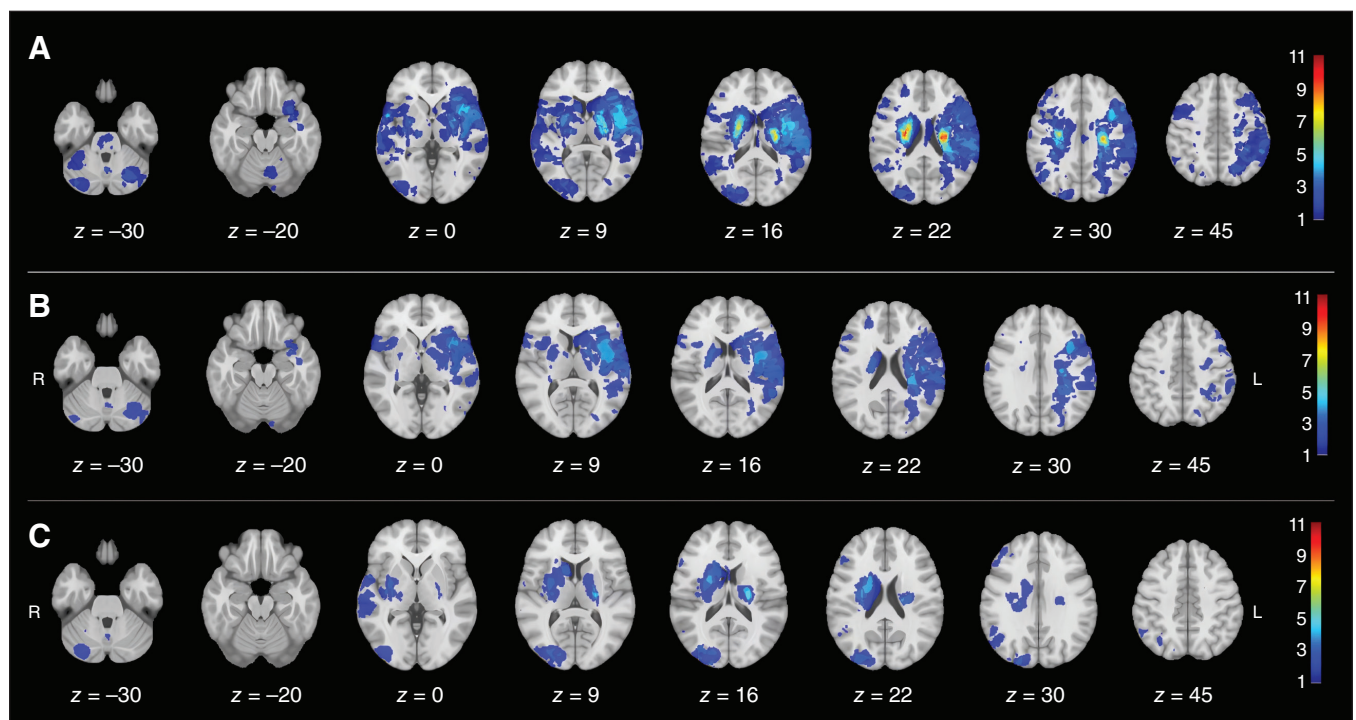


Figure 1: Distribution of infarct lesions in (A) the whole sample, (B) the low-empathy group, and (C) the high-empathy group. The prevalence of the infarct is colour-coded and superimposed on a 1-mm Montreal Neurological Institute 152 template. The colour bar indicates the number of patients with a lesion for each voxel.

Table 3: Univariate analysis of categorized empathy and brain atrophy

Structure	Atrophy ratio, %, mean ± SD			p value
	Low empathy	Moderate empathy	High empathy	
Left frontal lobe	40.44 ± 8.96	39.19 ± 7.51	36.47 ± 5.06	0.2
Right frontal lobe	37.50 ± 6.40	36.49 ± 7.71	34.46 ± 5.22	0.3
Left occipital lobe	15.32 ± 4.29	14.41 ± 4.27	12.28 ± 3.14	0.05
Right occipital lobe	11.42 ± 3.88	11.21 ± 3.84	9.25 ± 2.30	0.09
Left temporal lobe	31.99 ± 7.46	30.97 ± 6.72	27.26 ± 3.67	0.04
Right temporal lobe	21.35 ± 3.93	22.26 ± 4.94	19.63 ± 3.03	0.08
Left parietal lobe	40.55 ± 7.90	41.35 ± 11.10	37.04 ± 8.59	0.3
Right parietal lobe	36.16 ± 5.94	36.42 ± 8.68	32.73 ± 8.00	0.2
Left cingulate	10.68 ± 3.29	11.28 ± 10.08	7.78 ± 1.58	0.2
Right cingulate	16.20 ± 4.22	14.15 ± 3.05	13.02 ± 2.20	0.007
Left insula	31.10 ± 12.24	32.03 ± 18.61	23.53 ± 8.98	0.1
Right insula	21.42 ± 7.56	23.18 ± 10.46	17.51 ± 6.01	0.07
Cerebellum	9.54 ± 2.22	9.95 ± 2.17	9.72 ± 3.11	0.8
Left MTL	0.54 ± 0.16	0.56 ± 0.28	0.42 ± 0.14	0.07
Right MTL	0.50 ± 0.18	0.52 ± 0.28	0.39 ± 0.13	0.09

MTL = medial temporal lobe; SD = standard deviation.

Table 4: Univariate analysis of categorized empathy and total brain structure volumetry

Brain structure	Volume, mL, mean ± SD			p value
	Low empathy	Moderate empathy	High empathy	
ICV	1444.83 ± 131.93	1444.13 ± 122.06	1420.42 ± 132.91	0.8
Brain parenchyma	1099.62 ± 101.93	1082.26 ± 193.55	1116.73 ± 107.34	0.7
Hippocampus	6.64 ± 0.54	6.81 ± 0.72	6.97 ± 0.58	0.2
Amygdala	3.72 ± 0.31	3.72 ± 0.44	3.74 ± 0.37	1.0
Thalamus	11.31 ± 2.56	11.71 ± 1.22	12.40 ± 1.13	0.1
Caudate	6.68 ± 0.91	6.79 ± 0.92	6.76 ± 0.98	0.9
Putamen	10.19 ± 1.61	10.51 ± 1.27	10.83 ± 1.12	0.3
Pallidum	3.08 ± 0.52	3.04 ± 0.41	3.19 ± 0.39	0.5
Accumbens	1.06 ± 0.09	1.06 ± 0.16	1.10 ± 0.11	0.4
Hypothalamus	0.70 ± 0.06	0.69 ± 0.09	0.69 ± 0.07	0.9
Midbrain	5.90 ± 0.54	5.85 ± 0.62	6.07 ± 0.65	0.4
Pons	13.90 ± 1.30	13.65 ± 2.11	14.23 ± 1.75	0.5
Medulla	4.31 ± 0.37	4.19 ± 0.50	4.46 ± 0.50	0.1
SCP	0.22 ± 0.02	0.22 ± 0.03	0.22 ± 0.03	0.8
Cerebellum	134.27 ± 7.80	132.12 ± 13.34	132.85 ± 14.56	0.8

ICV = intracranial volume; SCP = superior cerebellar peduncle; SD = standard deviation.

We also conducted an analysis of fibre connections between the infarcted regions in the left cortex and the right cingulate areas (Figure 4). We found extensive fibrous linkages between the ischemic cortex region in the left hemisphere and the right cingulate.

Discussion

In this study, we identified structural abnormalities among patients with impaired empathy following stroke and investigated the corresponding changes in functional connectivity. Our main findings showed that severe atrophy of the right cingulate was associated with low empathy, while functional connectivity between the anterior division of the cingulate

gyrus and the right superior parietal lobule was relatively high in the low empathy group. This may represent a compensatory mechanism among patients with empathy impairment following ischemic stroke.

Although some patients exhibited higher EQ scores than controls, on average, patients with stroke tended to have lower EQ scores, indicative of poor empathy capabilities. This finding aligns with previous research, suggesting that stroke can complicate cognitive and emotional empathy impairments, even extending to disruptions in emotional processing abilities, ultimately contributing to poor outcomes.⁵

We found that the amygdala’s volume did not significantly correlate with reduced empathy. Conversely, an fMRI

Table 5: Univariate analysis of categorized empathy and unilateral brain volumetry

Brain structure	Volume, mL, mean \pm SD			<i>p</i> value
	Low empathy	Moderate empathy	High empathy	
Left hippocampus	3.26 \pm 0.22	3.33 \pm 0.41	3.39 \pm 0.29	0.5
Right hippocampus	3.38 \pm 0.35	3.46 \pm 0.37	3.58 \pm 0.31	0.2
Left amygdala	1.86 \pm 0.16	1.86 \pm 0.22	1.85 \pm 0.20	1.0
Right amygdala	1.86 \pm 0.17	1.87 \pm 0.24	1.89 \pm 0.17	0.9
Left lateral ventricle	15.77 \pm 6.35	19.32 \pm 15.26	12.81 \pm 9.27	0.1
Right lateral ventricle	14.61 \pm 8.24	15.66 \pm 11.48	9.73 \pm 6.78	0.08
Left inferior angle of the lateral ventricle	1.76 \pm 0.51	1.83 \pm 0.78	1.41 \pm 0.45	0.06
Right inferior angle of the lateral ventricle	1.73 \pm 0.72	1.76 \pm 0.81	1.38 \pm 0.47	0.1
Left thalamus	5.91 \pm 0.64	5.87 \pm 0.59	6.16 \pm 0.59	0.2
Right thalamus	5.86 \pm 0.88	5.85 \pm 0.69	6.24 \pm 0.63	0.1
Left caudate	3.42 \pm 0.42	3.44 \pm 0.42	3.50 \pm 0.40	0.8
Right caudate	3.40 \pm 0.88	3.34 \pm 0.56	3.26 \pm 0.62	0.8
Left putamen	4.91 \pm 0.91	5.16 \pm 0.74	5.30 \pm 0.48	0.2
Right putamen	5.27 \pm 0.90	5.42 \pm 0.78	5.53 \pm 0.71	0.6
Left pallidum	1.60 \pm 0.30	1.58 \pm 0.22	1.63 \pm 0.23	0.8
Right pallidum	1.76 \pm 1.37	1.46 \pm 0.21	1.56 \pm 0.22	0.3
Left accumbens	0.53 \pm 0.05	0.53 \pm 0.08	0.56 \pm 0.06	0.4
Right accumbens	0.53 \pm 0.06	0.53 \pm 0.08	0.55 \pm 0.06	0.4
Left hypothalamus	0.34 \pm 0.03	0.34 \pm 0.04	0.33 \pm 0.03	0.8
Right hypothalamus	0.36 \pm 0.04	0.36 \pm 0.04	0.36 \pm 0.04	0.9

SD = standard deviation.

Table 6: Total brain structure volumetry among patients after stroke and healthy controls

Brain structure	Volume, mL, mean \pm SD		<i>p</i> value
	Post-stroke patients <i>n</i> = 84	Healthy controls <i>n</i> = 22	
ICV	1438.66 \pm 112.57	1369.01 \pm 126.15	0.0
Brain parenchyma	1095.01 \pm 83.52	1068.28 \pm 154.84	0.4
Hippocampus	6.80 \pm 0.57	6.57 \pm 0.65	0.1
Amygdala	3.73 \pm 0.39	3.47 \pm 0.39	0.007
Thalamus	11.77 \pm 0.99	12.01 \pm 1.68	0.5
Caudate	6.75 \pm 1.01	6.42 \pm 0.92	0.1
Putamen	10.50 \pm 0.87	10.61 \pm 1.34	0.7
Pallidum	3.09 \pm 0.34	3.23 \pm 0.43	0.2
Accumbens	1.07 \pm 0.13	1.04 \pm 0.13	0.3
Hypothalamus	0.69 \pm 0.06	0.66 \pm 0.08	0.03
Midbrain	5.91 \pm 0.74	5.76 \pm 0.61	0.3
Pons	13.85 \pm 2.01	13.97 \pm 1.84	0.8
Medulla	4.29 \pm 0.56	4.26 \pm 0.48	0.8
SCP	0.22 \pm 0.03	0.21 \pm 0.03	0.04
Cerebellum	132.86 \pm 11.62	126.64 \pm 12.35	0.04

ICV = intracranial volume; SCP = superior cerebellar peduncle; SD = standard deviation.

experiment demonstrated that people whose amygdala was more robustly interconnected to brain regions had more intricate social networks than those with weaker intrinsic connectivity.²² This suggests that the amygdala operates as a central node within these complex networks, leveraging targeted connections to exert its influence, thereby transcending its mere anatomic role.

In contrast to our pilot study, which found a correlation between low EQ scores, small putamen volumes, and a high prevalence of right cortical infarcts,⁶ our current investigation found an association between low empathy and a high incidence of cerebral infarction in the left cortical region. This observation may stem from the expanded sample size and the adoption of alternative statistical methods. Notably,

Table 7: Univariate analysis of categorized empathy and structural connectivity

Brain structure	Fractional anisotropy, mean ± SD				Diffusivity, mean ± SD			
	Low empathy	Moderate empathy	High empathy	p value	Low empathy	Moderate empathy	High empathy	p value
MCP	0.56 ± 0.04	0.57 ± 0.03	0.56 ± 0.03	0.5	0.75 ± 0.07	0.74 ± 0.05	0.74 ± 0.05	0.9
PCT	0.51 ± 0.07	0.49 ± 0.07	0.51 ± 0.05	0.5	0.75 ± 0.09	0.80 ± 0.14	0.77 ± 0.09	0.3
GCC	0.59 ± 0.03	0.59 ± 0.05	0.61 ± 0.04	0.2	0.85 ± 0.10	0.85 ± 0.10	0.81 ± 0.07	0.2
BCC	0.57 ± 0.07	0.57 ± 0.10	0.63 ± 0.05	0.04	1.00 ± 0.18	1.02 ± 0.33	0.88 ± 0.09	0.1
SCC	0.64 ± 0.10	0.63 ± 0.11	0.66 ± 0.04	0.4	0.96 ± 0.15	1.01 ± 0.35	0.90 ± 0.10	0.3
FX	0.44 ± 0.08	0.44 ± 0.09	0.52 ± 0.10	0.004	1.72 ± 0.29	1.70 ± 0.32	1.46 ± 0.37	0.02
Right CST	0.58 ± 0.06	0.56 ± 0.07	0.56 ± 0.04	0.6	0.75 ± 0.04	0.77 ± 0.08	0.77 ± 0.06	0.6
Left CST	0.57 ± 0.09	0.58 ± 0.06	0.57 ± 0.05	0.8	0.78 ± 0.12	0.77 ± 0.08	0.76 ± 0.06	0.8
Right ML	0.62 ± 0.08	0.61 ± 0.07	0.61 ± 0.03	0.9	0.76 ± 0.05	0.77 ± 0.11	0.77 ± 0.03	1.0
Left ML	0.61 ± 0.10	0.62 ± 0.06	0.61 ± 0.03	0.9	0.78 ± 0.15	0.76 ± 0.08	0.76 ± 0.04	0.6
Right ICP	0.57 ± 0.05	0.57 ± 0.05	0.57 ± 0.04	0.9	0.76 ± 0.06	0.77 ± 0.08	0.75 ± 0.03	0.8
Left ICP	0.56 ± 0.08	0.58 ± 0.05	0.57 ± 0.03	0.5	0.82 ± 0.14	0.77 ± 0.11	0.77 ± 0.03	0.2
Right SCP	0.68 ± 0.08	0.68 ± 0.06	0.67 ± 0.02	0.9	0.96 ± 0.15	0.95 ± 0.06	0.97 ± 0.09	0.7
Left SCP	0.67 ± 0.11	0.68 ± 0.05	0.68 ± 0.02	0.8	0.97 ± 0.10	0.96 ± 0.09	0.96 ± 0.07	0.8
Right CP	0.64 ± 0.07	0.65 ± 0.05	0.65 ± 0.03	0.9	0.84 ± 0.18	0.81 ± 0.14	0.78 ± 0.05	0.4
Left CP	0.63 ± 0.09	0.65 ± 0.06	0.66 ± 0.04	0.3	0.88 ± 0.30	0.80 ± 0.16	0.77 ± 0.05	0.2
Right ALIC	0.53 ± 0.08	0.53 ± 0.05	0.56 ± 0.04	0.2	0.77 ± 0.07	0.78 ± 0.08	0.74 ± 0.06	0.2
Left ALIC	0.50 ± 0.07	0.51 ± 0.06	0.53 ± 0.04	0.2	0.79 ± 0.12	0.78 ± 0.09	0.76 ± 0.08	0.5
Right PLIC	0.65 ± 0.03	0.65 ± 0.05	0.64 ± 0.04	0.7	0.71 ± 0.04	0.72 ± 0.04	0.72 ± 0.03	0.8
Left PLIC	0.65 ± 0.04	0.65 ± 0.04	0.64 ± 0.05	0.3	0.72 ± 0.05	0.72 ± 0.04	0.74 ± 0.07	0.4
Right RLIC	0.58 ± 0.08	0.60 ± 0.07	0.59 ± 0.04	0.5	0.87 ± 0.25	0.82 ± 0.17	0.79 ± 0.05	0.3
Left RLIC	0.59 ± 0.09	0.62 ± 0.04	0.61 ± 0.03	0.2	0.83 ± 0.19	0.79 ± 0.06	0.79 ± 0.04	0.4
Right ACR	0.41 ± 0.04	0.42 ± 0.06	0.44 ± 0.04	0.3	0.81 ± 0.07	0.83 ± 0.13	0.79 ± 0.07	0.3
Left ACR	0.40 ± 0.04	0.40 ± 0.05	0.42 ± 0.04	0.4	0.82 ± 0.08	0.84 ± 0.13	0.80 ± 0.07	0.4
Right SCR	0.48 ± 0.05	0.48 ± 0.06	0.49 ± 0.05	0.8	0.80 ± 0.12	0.82 ± 0.19	0.74 ± 0.06	0.1
Left SCR	0.47 ± 0.04	0.48 ± 0.06	0.49 ± 0.03	0.3	0.79 ± 0.08	0.83 ± 0.21	0.76 ± 0.07	0.2
Right PCR	0.45 ± 0.06	0.46 ± 0.06	0.47 ± 0.05	0.7	0.91 ± 0.22	0.92 ± 0.21	0.85 ± 0.09	0.4
Left PCR	0.44 ± 0.05	0.45 ± 0.06	0.45 ± 0.07	0.7	0.88 ± 0.14	0.92 ± 0.23	0.91 ± 0.34	0.8
Right PTR	0.57 ± 0.08	0.57 ± 0.08	0.58 ± 0.04	0.8	0.89 ± 0.18	0.89 ± 0.19	0.86 ± 0.06	0.7
Left PTR	0.56 ± 0.07	0.58 ± 0.05	0.59 ± 0.04	0.4	0.92 ± 0.18	0.91 ± 0.18	0.86 ± 0.06	0.4
Right SS	0.54 ± 0.09	0.55 ± 0.07	0.54 ± 0.04	0.9	0.92 ± 0.34	0.89 ± 0.25	0.86 ± 0.06	0.8
Left SS	0.54 ± 0.08	0.55 ± 0.04	0.55 ± 0.03	0.6	0.92 ± 0.24	0.87 ± 0.06	0.86 ± 0.05	0.3
Right EC	0.44 ± 0.04	0.45 ± 0.05	0.45 ± 0.04	0.5	0.82 ± 0.10	0.80 ± 0.08	0.78 ± 0.05	0.3
Left EC	0.44 ± 0.05	0.45 ± 0.05	0.46 ± 0.03	0.2	0.83 ± 0.13	0.81 ± 0.08	0.79 ± 0.05	0.4
Right CGC	0.49 ± 0.04	0.49 ± 0.06	0.51 ± 0.04	0.3	0.77 ± 0.10	0.79 ± 0.24	0.75 ± 0.03	0.7
Left CGC	0.49 ± 0.05	0.49 ± 0.07	0.51 ± 0.04	0.7	0.78 ± 0.14	0.80 ± 0.29	0.75 ± 0.03	0.7
Right CGH	0.48 ± 0.05	0.48 ± 0.05	0.48 ± 0.04	1.0	0.82 ± 0.14	0.81 ± 0.15	0.79 ± 0.03	0.7
Left CGH	0.48 ± 0.05	0.48 ± 0.04	0.48 ± 0.03	0.9	0.89 ± 0.26	0.84 ± 0.18	0.81 ± 0.04	0.3
Right FX/ST	0.49 ± 0.08	0.51 ± 0.06	0.53 ± 0.05	0.1	1.11 ± 0.25	1.07 ± 0.18	0.99 ± 0.12	0.1
Left FX/ST	0.54 ± 0.05	0.55 ± 0.05	0.56 ± 0.04	0.4	0.89 ± 0.17	0.87 ± 0.08	0.86 ± 0.05	0.6
Right SLF	0.49 ± 0.04	0.49 ± 0.07	0.50 ± 0.04	0.6	0.76 ± 0.07	0.77 ± 0.08	0.74 ± 0.04	0.3
Left SLF	0.47 ± 0.05	0.48 ± 0.06	0.50 ± 0.03	0.1	0.74 ± 0.07	0.77 ± 0.12	0.74 ± 0.05	0.3
Right SFO	0.45 ± 0.08	0.45 ± 0.07	0.45 ± 0.09	1.0	0.85 ± 0.22	0.86 ± 0.18	0.81 ± 0.12	0.6
Left SFO	0.39 ± 0.07	0.41 ± 0.07	0.44 ± 0.06	0.05	0.91 ± 0.13	0.91 ± 0.20	0.81 ± 0.10	0.08
Right IFO	0.53 ± 0.04	0.54 ± 0.04	0.54 ± 0.03	0.5	0.80 ± 0.07	0.80 ± 0.06	0.79 ± 0.03	0.7
Left IFO	0.49 ± 0.05	0.51 ± 0.05	0.52 ± 0.04	0.1	0.81 ± 0.07	0.80 ± 0.06	0.79 ± 0.04	0.5
Right UNC	0.51 ± 0.06	0.54 ± 0.05	0.53 ± 0.04	0.2	0.78 ± 0.04	0.76 ± 0.05	0.77 ± 0.04	0.08
Left UNC	0.50 ± 0.06	0.53 ± 0.06	0.55 ± 0.04	0.05	0.81 ± 0.19	0.77 ± 0.06	0.76 ± 0.04	0.2
Right TAP	0.40 ± 0.08	0.39 ± 0.09	0.45 ± 0.07	0.04	1.74 ± 0.32	1.83 ± 0.31	1.54 ± 0.24	0.002
Left TAP	0.35 ± 0.09	0.36 ± 0.07	0.40 ± 0.09	0.09	1.96 ± 0.38	1.99 ± 0.27	1.77 ± 0.34	0.04

ACR = anterior corona radiata; ALIC = anterior limb of the internal capsule; BCC = body of the corpus callosum; CGC = cingulum (cingulate gyrus); CGH = cingulum (hippocampus); CP = cerebral peduncle; CST = corticospinal tract; EC = external capsule; FX = fornix; FX/ST = fornix (cross)/stria terminalis (can not be resolved with current resolution); GCC = genu of the corpus callosum; ICP = inferior cerebellar peduncle; IFO = inferior fronto-occipital fasciculus; MCP = middle cerebellar peduncle; ML = medial lemniscus; PCR = posterior corona radiata; PCT = pontine crossing tract (part of the MCP); PLIC = posterior limb of the internal capsule; PTR = posterior thalamic radiation (including optic radiation); RLIC = retrolenticular part of internal capsule; SCC = splenium of the corpus callosum; SCR = superior corona radiata; SCP = superior cerebellar peduncle; SD = standard deviation; SFO = superior fronto-occipital fasciculus (could be a part of the anterior internal capsule); SLF = superior longitudinal fasciculus; SS = sagittal stratum (including inferior longitudinal fasciculus and inferior fronto-occipital fasciculus); TAP = tapetum; UNC = uncinata fasciculus.

our findings in the 2 studies both suggested that poor empathy was associated with high incidence of cortical infarctions, affecting not only the left hemisphere (29.8% in current study, 24.4% in pilot study) but also the right hemisphere (26.2% in current study, 19.5% in pilot study). These results underscore the crucial role of an intact hemispheric cortex in empathy processes. From a neuroanatomical perspective, empathy relies on numerous cortical areas and their connectivity. For instance, with frontotemporal dementia, loss of grey matter occurs mainly in the left frontal lobes — particularly in the orbital, medial, and dorsolateral regions — followed by the temporal lobes, resulting in empathy deficits.^{23,24}

Table 8: Multivariate binary logistic regression of putative risk factors for low empathy

Variable	β	OR (95% CI)	R^2
Model 1			
Atrial fibrillation	1.266	3.547 (0.472–26.688)	
Left cortical infarct	1.407	4.082 (1.183–14.088)	
Atrophy of right cingulate	0.222	1.248 (1.038–1.502)	
Mean diffusivity of right tapetum	–1.429	0.240 (0.039–1.473)	
MoCA	–0.178	0.837 (0.740–0.947)	
Model 2*			
Fractional anisotropy of fornix	2.086	8.050 (0.008–8405.634)	0.41

CI = confidence interval; MoCA = Montreal Cognitive Assessment; OR = odds ratio.
*Model 2 replaced the mean diffusivity of the right tapetum with the fractional anisotropy of the fornix, while holding all other variables in model 1 as constant.

We found that low fractional anisotropy or high mean diffusivity within specific brain regions may be correlated with poor empathy, such as the fornix and tapetum. This finding suggests the presence of structural connectivity impairments in various brain structures among patients following stroke, which may be linked to empathy impairment. Notably, the fornix serves as a pivotal component within the limbic system and plays a vital coordinating role in the Papez circuit.²⁵ Damage to these structures can lead to conduct disorder and elevated callous or unemotional traits, in addition to cognitive impairments.²⁶ Although our regression model did not find a significant correlation between structural connectivity features and low empathy, further exploration of the intricate relationship between structural connectivity and empathy necessitates the incorporation of more comprehensive functional information and connectivity-based analytical models.

We also found that a lower MoCA score was associated with low empathy. People with cortical neurodegenerative diseases such as Alzheimer disease and frontotemporal dementia often have declines in both cognitive and emotional elements of empathy. Emotion recognition involves the interaction of shared neural representation, self-awareness, mental flexibility, and emotion regulation.²⁷ A decline in cognitive function could impair emotional processes, leading to altered empathy.

As the presence of more left cortical infarcts is associated with decreased empathy, it is intriguing and somewhat surprising to observe that atrophy of the right cingulate, but not the ipsilateral one, is more predisposed to impaired empathy. Atrophy of the right cingulate cortex may be correlated with pre-existing abnormalities, which could

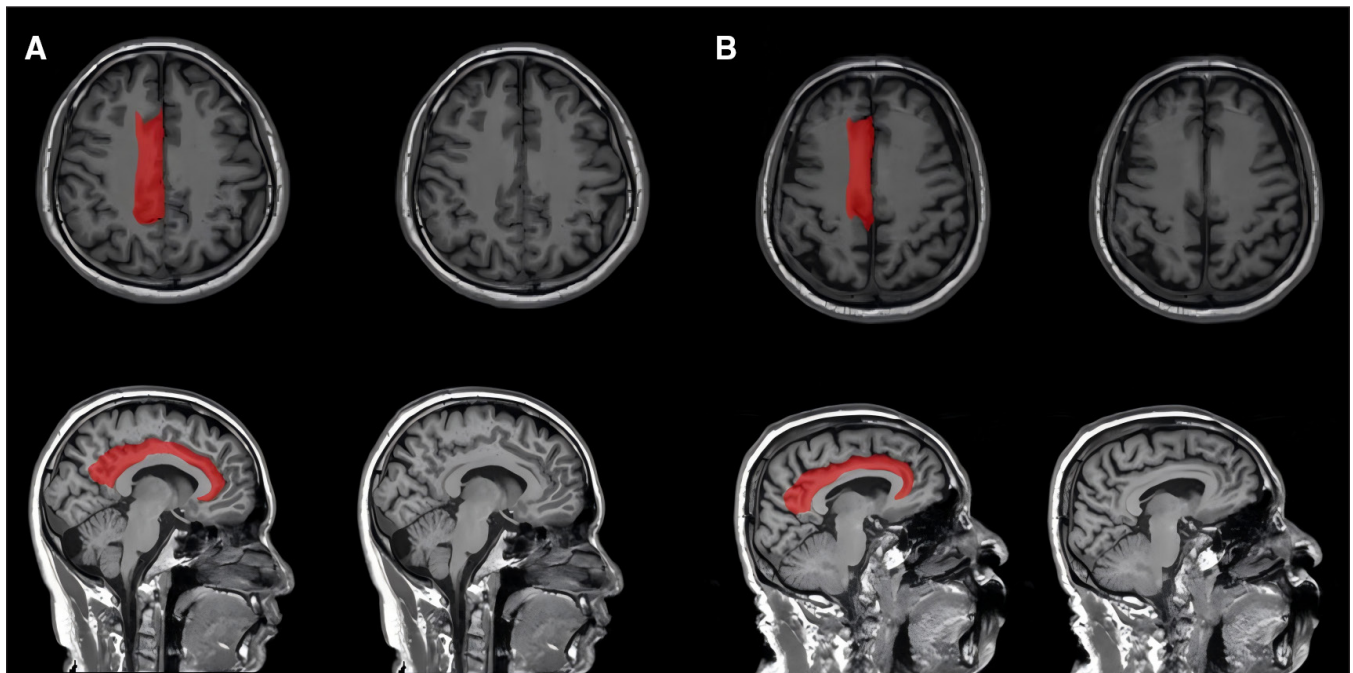


Figure 2: The quantification the right cingulate atrophy among patients with different levels of empathy. (A) A 74-year-old patient with an empathy quotient (EQ) of 28 (low empathy) at 3 months after stroke and a large right cingulate atrophy ratio of 25.4%. (B) A 34-year-old patient with an EQ of 75 (high empathy) at 3 months after stroke and a smaller right cingulate atrophy ratio of 12.2%.

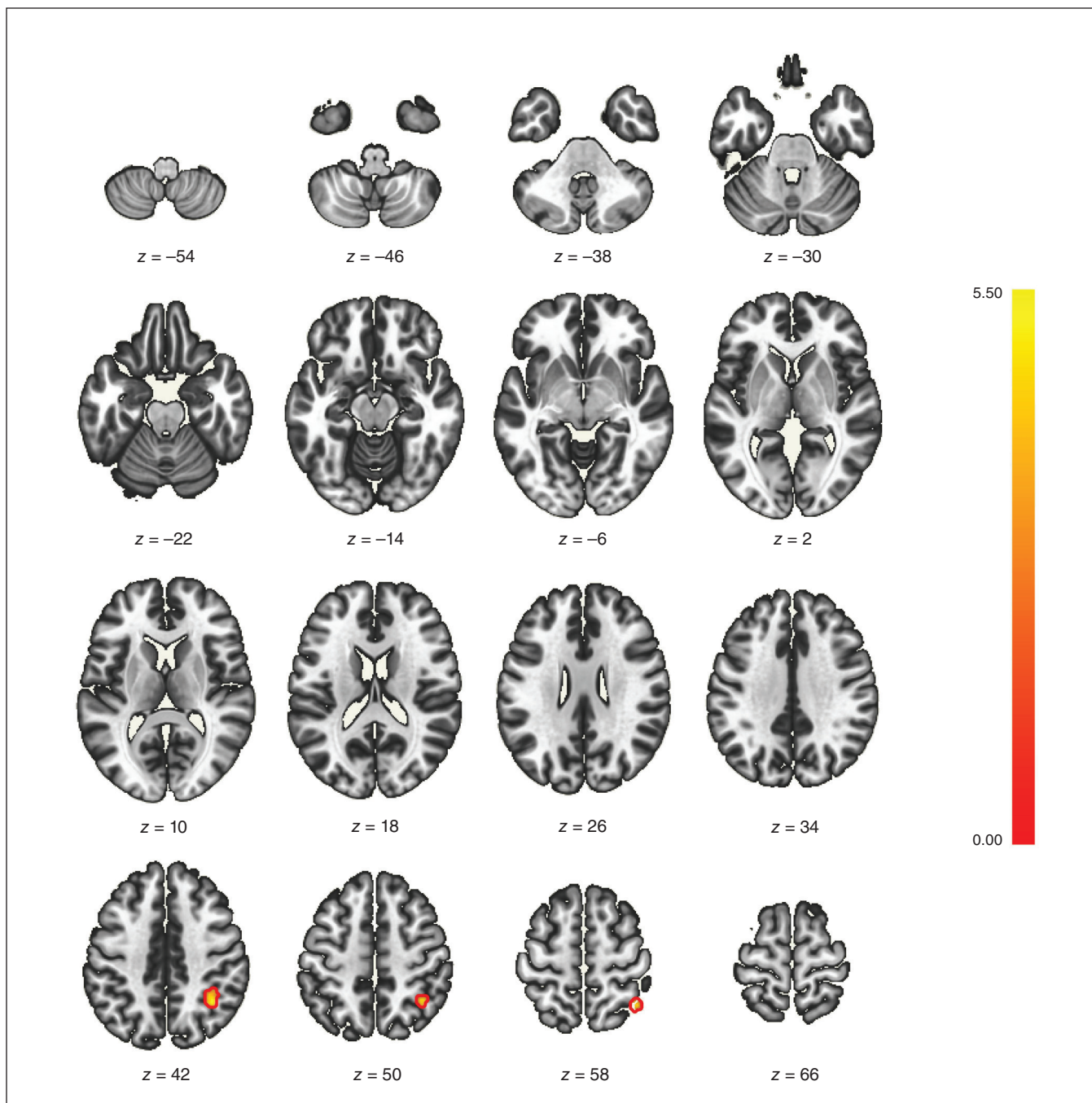


Figure 3: The seed-based functional magnetic resonance imaging analysis between patients with low or high empathy after stroke. On the cluster +36 (x), -50 (y), +44 (z), 136 (69%) voxels covered 9% of the right superior parietal lobule, 28 (14%) voxels covered 2% of the right angular gyrus, 9 (5%) voxels covered 1% of the right superior lateral occipital cortex, and 7 (4%) voxels covered 1% of the right posterior supramarginal gyrus.

potentially lead to reduced brain reserve. In addition, it may be secondary to the index acute ischemic stroke. To further investigate this phenomenon, we conducted an analysis of fibre connections between the infarcted regions in the left cortex and the right cingulate areas. Based on our findings of extensive fibrous linkages between the ischemic cortex region in the left hemisphere and the right cingulate,

we hypothesize that ischemic damage may play a pivotal role in the atrophy process, particularly affecting the right cingulate gyrus, which could subsequently contribute to the observed decline in empathy. Since the cingulate cortex is a crucial component of the neural network involved in empathy processing,¹⁰ these changes could subsequently contribute to the observed decline in empathy.

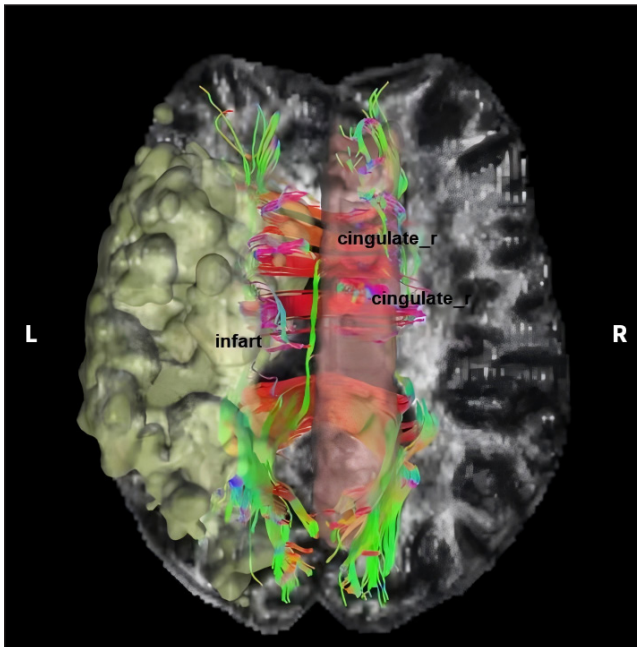


Figure 4: Schematic diagram of fibre connections between a left cortical infarct and the right cingulate gyrus. A left cortical infarct is shown in yellow, the right cingulate is shown in pink, left–right fibres are shown as red lines, anterior–posterior fibres are shown as green lines, and superior–inferior fibres are shown as blue lines.

We observed increased functional connectivity between the anterior division of the cingulate gyrus and the right superior parietal lobule among patients with low empathy, suggesting a potential compensatory pattern for empathy impairment related to structural brain damage. Previous research has shown that the emotional component of empathy is linked to the mirror neuron system, while the cognitive component involves the inferior parietal lobule.⁹ Studies involving macaques have found cortico–cortical connections between the caudal superior parietal lobule and the posterior cingulate cortex.²⁸ Enhanced functional connectivity in the superior parietal lobule may facilitate the understanding of complex visual scenes and the simultaneous processing of multiple elements to ascertain a global meaning,²⁹ which may functionally compensate for the reduced empathy.

Limitations

Although we found that the severity of cingulate atrophy was associated with empathy, we did not specifically investigate ischemic cingulate lesions. We did not explore the relationship between specific network involvement and empathy impairment, which may limit the generalizability of our findings. Although we excluded patients with psychological disorders according to the medical records, we may have included patients who used antipsychotic medications at follow-up. However, we did not record the information about psychotropic medication. We did not test EQ or MoCA scores before the index stroke, which resulted in certain constraints in the derived conclusion.

Conclusion

Among patients who had experienced a subacute ischemic stroke, low empathy was strongly associated with a severe cognitive profile and atrophy of the right cingulate cortex. Structural-informed fMRI analysis found that enhanced connectivity between the anterior cingulate gyrus and the superior parietal lobule may function as a compensatory mechanism for this atrophy.

Affiliations: From the Department of Neurology, The Tenth Affiliated Hospital of Southern Medical University (Dongguan People's Hospital), Dongguan, Guangdong Province, China (Qu, Liu, Wang, Chen); the Faculty of Neurology, Graduate School of Guangdong Medical University, Zhanjiang, Guangdong Province, China (Qu, Liu); the Faculty of Neurology, Graduate School of Southern Medical University, Guangzhou, Guangdong Province, China (Wang); the BrainNow Research Institute, Shenzhen, Guangdong Province, China (Luo, Shi); the School of Mathematics and Statistics, Huazhong University of Science and Technology, China (Gao); the Center for Mathematical Science, Huazhong University of Science and Technology, China (Gao); the Intelligent Brain Imaging and Brain Function Laboratory (Dongguan Key Laboratory), Dongguan People's Hospital, Dongguan, Guangdong, China (Qu, Chen); the Guangdong Provincial Key Laboratory of Mathematical and Neural Dynamical Systems, Great Bay University, Dongguan, Guangdong, China (Qu, Gao, Chen).

Competing interests: Yi-Shan Luo is employed by BrainNow Medical Technology Limited. Lin Shi is the director of BrainNow Medical Technology. No other competing interests were declared.

Contributors: Jian-Feng Qu and Yang-Kun Chen contributed to the conception and design of the work. Jian-Feng Qu, Xiao-Wen Liu, Ming-Zi Wang, Yi-Shan Luo, Ting Gao, and Lin Shi contributed to data acquisition, analysis, and interpretation. Jian-Feng Qu drafted the manuscript. All of the authors revised it critically for important intellectual content, gave final approval of the version to be published, and agreed to be accountable for all aspects of the work.

Content licence: This is an Open Access article distributed in accordance with the terms of the Creative Commons Attribution (CC BY-NC-ND 4.0) licence, which permits use, distribution and reproduction in any medium, provided that the original publication is properly cited, the use is noncommercial (i.e., research or educational use), and no modifications or adaptations are made. See: <https://creativecommons.org/licenses/by-nc-nd/4.0/>

Funding: This study was supported by the Dongguan Science and Technology of Social Development Program (no. 20211800905182) and Guangdong Basic and Applied Basic Research Foundation (no. 2020B1515120055).

References

1. Adolphs R. Cognitive neuroscience of human social behaviour. *Nat Rev Neurosci* 2003;4:165-78.
2. Beaudoin C, Beauchamp MH. Social cognition. *Handb Clin Neurol* 2020;173:255-64.
3. Shamay-Tsoory SG, Tomer R, Goldsher D, et al. Impairment in cognitive and affective empathy in patients with brain lesions: anatomical and cognitive correlates. *J Clin Exp Neuropsychol* 2004;26:1113-27.
4. Henry JD, von Hippel W, Molenberghs P, et al. Clinical assessment of social cognitive function in neurological disorders. *Nat Rev Neurol* 2016;12:28-39.
5. Yeh ZT, Tsai CF. Impairment on theory of mind and empathy in patients with stroke. *Psychiatry Clin Neurosci* 2014;68:612-20.
6. Qu JF, Zhou YQ, Liu JF, et al. Right cortical infarction and a reduction in putamen volume may be correlated with empathy in patients after subacute ischemic stroke—a multimodal magnetic resonance imaging study. *J Clin Med* 2022;11:4479.

7. Stevens F, Taber K. The neuroscience of empathy and compassion in pro-social behavior. *Neuropsychologia* 2021;159:107925.
8. Ziaei M, Oestreich L, Persson J, et al. Neural correlates of affective empathy in aging: a multimodal imaging and multivariate approach. *Neuropsychol Dev Cogn B Aging Neuropsychol Cogn* 2022;29:577-98.
9. Bernhardt BC, Singer T. The neural basis of empathy. *Annu Rev Neurosci* 2012;35:1-23.
10. Fan Y, Duncan NW, de Greck M, et al. Is there a core neural network in empathy? An fMRI based quantitative meta-analysis. *Neurosci Biobehav Rev* 2011;35:903-11.
11. Cox CL, Uddin LQ, Di Martino A, et al. The balance between feeling and knowing: affective and cognitive empathy are reflected in the brain's intrinsic functional dynamics. *Soc Cogn Affect Neurosci* 2012;7:727-37.
12. Salvalaggio A, De Filippo De Grazia M, Zorzi M, et al. Post-stroke deficit prediction from lesion and indirect structural and functional disconnection. *Brain* 2020;143:2173-88.
13. Leigh R, Oishi K, Hsu J, et al. Acute lesions that impair affective empathy. *Brain* 2013;136:2539-49.
14. Kidwell CS, Warach S. Acute ischemic cerebrovascular syndrome: diagnostic criteria. *Stroke* 2003;34:2995-8.
15. Adams HP Jr, Bendixen BH, Kappelle LJ, et al. Classification of subtype of acute ischemic stroke. Definitions for use in a multicenter clinical trial. *Stroke* 1993;24:35-41.
16. Zhao Q, Neumann DL, Cao X, et al. Validation of the empathy quotient in mainland China. *J Pers Assess* 2018;100:333-42.
17. Baron-Cohen S, Wheelwright S. The empathy quotient: an investigation of adults with Asperger syndrome or high functioning autism, and normal sex differences. *J Autism Dev Disord* 2004;34:163-75.
18. Nasreddine ZS, Phillips NA, Bédirian V, et al. The Montreal Cognitive Assessment, MoCA: a brief screening tool for mild cognitive impairment. *J Am Geriatr Soc* 2005;53:695-9.
19. Abrigo J, Shi L, Luo Y, et al.; Alzheimer's Disease Neuroimaging Initiative. Standardization of hippocampus volumetry using automated brain structure volumetry tool for an initial Alzheimer's disease imaging biomarker. *Acta Radiol* 2019;60:769-76.
20. Mori S, Oishi K, Jiang H, et al. Stereotaxic white matter atlas based on diffusion tensor imaging in an ICBM template. *Neuroimage* 2008;40:570-82.
21. Whitfield-Gabrieli S, Nieto-Castanon A. Conn: a functional connectivity toolbox for correlated and anticorrelated brain networks. *Brain Connect* 2012;2:125-41.
22. Bickart KC, Hollenbeck MC, Barrett LF, et al. Intrinsic amygdala-cortical functional connectivity predicts social network size in humans. *J Neurosci* 2012;32:14729-41.
23. Preston SD, de Waal FB. Empathy: its ultimate and proximate bases. *Behav Brain Sci* 2002;25:1-20.
24. Whitwell JL, Weigand SD, Boeve BF, et al. Neuroimaging signatures of frontotemporal dementia genetics: C9ORF72, tau, progranulin and sporadics. *Brain* 2012;135:794-806.
25. Lövblad KO, Schaller K, Vargas MI. The fornix and limbic system. *Semin Ultrasound CT MR* 2014;35:459-73.
26. Puzzo J, Seunarine K, Sully K, et al. Altered white-matter microstructure in conduct disorder is specifically associated with elevated callous-unemotional traits. *J Abnorm Child Psychol* 2018;46:1451-66.
27. Fortier J, Besnard J, Allain P. Theory of mind, empathy and emotion perception in cortical and subcortical neurodegenerative diseases. *Rev Neurol (Paris)* 2018;174:237-46.
28. Gamberini M, Passarelli L, Fattori P, et al. Structural connectivity and functional properties of the macaque superior parietal lobule. *Brain Struct Funct* 2020;225:1349-67.
29. Vialatte A, Yeshurun Y, Khan AZ, et al. Superior parietal lobule: a role in relative localization of multiple different elements. *Cereb Cortex* 2021;31:658-71.